NASA TM- 77494

NASA TECHNICAL MEMORANDUM

NASA TM-77494

TURBULENT BOUNDARY LAYERS WITH SECONDARY FLOW

E. Grushwitz

(NASA-TM-77494) TURBULENT BOUNDARY LAYERS WITH SECONDARY FLOW (National Aeronautics and Space Administration) 19 p
HC A02/MF A01 CSCL 20D

N85-13176

Unclas
G3/34 24499

Translation of "Turbulente Reibungsschichten mit Sekundärströmung", Ingenieur-Archiv, Vol. 6., 1935, pp. 355-365.

NATIONAL AERONAUTICS AND SPACE ADMINISTRATION
WASHINGTON, D.C. 20546 JULY 1984

STANDARD TITLE PAGE

1. Report No. NASA TM-77494	2. Government Accession No.	3. Recipient's Catalog No.
4. Title and Subtitle TURBULENT BOUNDARY LAYERS WITH SECONDARY FLOW.		5. Report Date July 1984 6. Performing Organization Code
7. Author(s) E. Grushwitz Kaiser Wilhelm Institute for Flow Research in Göttingen.		8. Performing Organization Report No. 10. Work Unit No.
9. Performing Organization Name and Address Leo Kanner Associates Redwood City, California, 20546		11. Contract or Grant No. NASw-3541 13. Type of Report and Period Covered Translation
12. Sponsoring Agency Name and Address National Aeronautics and Space Administration, Washington, D.C. 20546		14. Sponsoring Agency Code

15. Supplementary Notes

Translation of "Turbulente Reibungsschichten mit Sekundärströmung", Ingenieur-Archiv, Vol. 6, 1935, pp. 355-365.

16. Abstract The article describes measurements with an experimental equipment used to study the boundary layer on a plane wall, along which the flow occurs, whose potential flow lines are curved in plane parallel to the wall. According to the equation frequently applied to boundary layers in a plane flow, which is usually obtained there by using the pulse law, a generalization is derived which is valid for boundary layers with spatial flow. The wall shear stresses were calculated with this equation.

(Received June 5, 1935).

17. Key Words (Selected by Author(s))	18. Distribution Statement Unclassified-Unlimited		
19. Security Classif. (of this report) Unclassified	20. Security Classif. (of this page) Unclassified	21. No. of Pages 19	22.

N85-13176#

TURBULENT BOUNDARY LAYERS WITH SECONDARY FLOW

E. Grushwitz

The previous publications on friction layers or boundary layers[1] concern almost exclusively bidimensional flow processes, but naturally the processes with rotation symmetry have also been studied. This study represents an attempt to learn experimentally something about the processes in a boundary layer with three-dimensional flow, and specifically the boundary layer is studied on a plane wall, along which a flow occurs, whose potential flow lines are curved in planes parallel to the wall. A pressure gradient directed perpendicularly to the flow line on its concave side and lying in the plane of curvature corresponds to a flow line curvature. Since the static pressure in the boundary layer is mainly the same as in the limiting potential flow, the flow line in the boundary layer, because of the lower velocities occurring there may be curved more strongly than the potential flow lines, or assume a different direction from them. The flow lines in the boundary layer are consequently deflected more toward the inside, the closer they are to the wall. The name secondary flow has been given to the component arriving there perpendicular to the direction of the potential velocity. /355*

In view of the difficulties arising in the comparison of spatial flows according to their mathematical treatment, and since very little is known up to now about the turbulence mechanism,

---

[1]For the region adjacent to a body surrounded by flow, in which the decrease of velocity to zero takes place, the author uses, to satisfy the wish of Professor Prandtl, the word "friction layer" instead of the "boundary layer" commonly used in the literature. The boundary layer will designate the laminar component of the friction layer.

*Numbers in the margin indicate pagination in the foreign text.

there is hardly any prospect of mastering even approximately these complicated processes under the theoretical aspect within a foreseeable time. The measurements described in this article are therefore carried out to obtain an indication of the order of magnitude of the effects occurring in this connection.

I have to thank Professor Prandtl for suggesting this work and the Cooperative Aid Association of German Science for making it possible.

1. Experiments

1. The experimental channel. The experimental equipment (see Fig. 1) consisted of a channel of rectangular cross section, which had first a straight piece 1 m long. This was followed by a channel piece curved by 90°, the diameter of curvature of the internal channel wall was 45 cm, that on the external wall 90 cm. The boundary layer of the upper plane channel was studied. For this purpose in this channel wall, consisting of 5 mm thick iron plate, holes were provided, whose position is apparent from Figs. 1 and 5 (circles in Fig. 1). These holes were provided with thread, in which it was possible to screw a shifting device called the measurement equipment used to study the boundary layer. The unused holes were sealed with screw plugs, which closed flush with the internal channel wall. In the places (points) shown in Fig. 1, holes were also provided to measure static pressure. Air was blown through the channel by means of a blower in the direction /356 indicated by the arrow. Between the blower and the experimental section a rectifier, several sieves and a 2.5 m long stabilizing channel were installed. The pressure in the stabilizing channel and therefore the wind velocity were kept unaltered through a Schrenk regulator[2]. The blower was the same as used earlier by the author to measure boundary layers in a plane flow[3]. Just as in

---

[2]Compare O. Schrenk, Ing.-Arch. 1, 350 (1930).
[3]E. Gruschwitz, Ing.-Arch 2, 321 (1931).

the case of those measurements, here too a slit was provided in front of the measurement plate, through which the friction layer coming from the wall of the stabilizing channel was able to flow out of the channel, so that a new boundary layer began on the measurement plate. As shown by Fig. 1, the experimental channel had in its front part a small extension and from then on its cross section remained the same (45 cm wide, 50 cm high). The extension was installed for the purpose of allowing the boundary layer at the measurement plate to become turbulent as soon as possible.

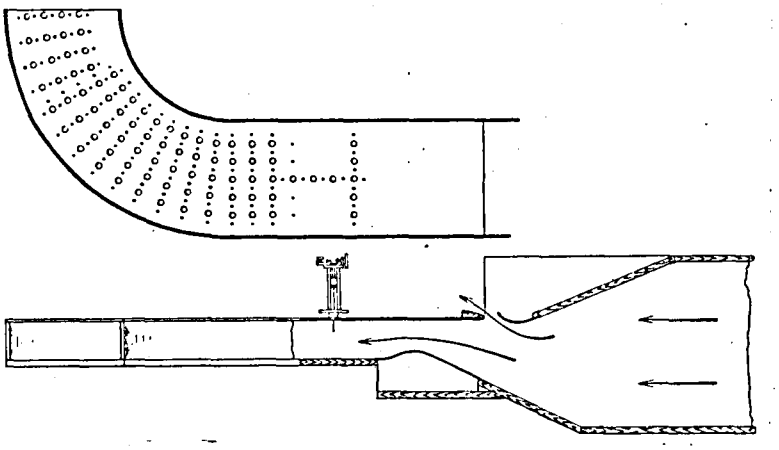

Figure 1. The experimental channel and measurement plate (measurement plate seen from below).

2. The measurement instrument. In the boundary layer to be studied there are mainly two velocity components: specifically the two components parallel to the wall. The third, perpendicular to the wall is so small as compared with the other two, that it may be considered negligible for the measurement. Therefore measurement equipment had to be used, which allowed the measurement of these two components or with which the value of the velocity of the wind and its direction could be measured. As such an instrument a thin cylindrical tube was used, which could be shifted perpendicularly to the wall in the flow, through a hole in the wall on which the boundary layer was to be measured. In

this tube three holes were provided near each other in a plane perpendicular to the tube axis. The tube was turned until both external holes showed the same pressure, by which the direction of the velocity of the wind was determined. Then the total pressure was measured with a third hole. The free end of the cylinder tube was closed with a hemisphere, whose diameter was equal to the cylinder diameter.

To obtain a survey of the variation of pressure at the end of the tube, a similar larger one was first built, whose diameter was 11.8 mm. In it pressure measurement holes were provided in the places indicated in Fig. 2. The cylindrical tube was brought into an air flow in such a way that the generator on which the pressure measurement holes lay became the straight line of stagnation. In Fig. 2 the measured pressure q_z, refer to the pressure head q_o of the undisturbed flow as plotted over the distance from the tube end. The blowing speed was in this case 20.5 m/sec. /357

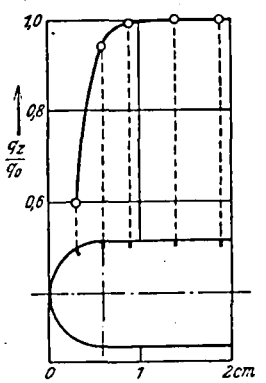

Figure 2. Pressure distribution along the straight line of stagnation of a cylindrical tube with hemispheric end with flow perpendicular to its axis.

The position of the holes in the tube used finally for the measurements may be seen in Fig. 3. The pressure at both external holes was sent upwards through the measurement tube through thin steel tubes (internal diameter 0.4 mm, external diameter 0.6 mm) through the measurement tube, while the central hole ended directly in the measurement tube. The external holes were connected with an oblique U-shaped tube, the central one to a Prandtl manometer. Both thin steel tubes gave rise unfortunately to fairly long adjustment time.

The central hole did not show fully the total pressure head, therefore a calibration factor must be taken into consideration. If the indication of the cylindrical tube is designated by q_z and

the pressure head by q, then, as shown by comparison with a pitot tube, $q=1.028q_z$.

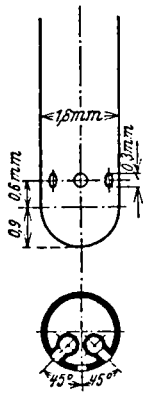

Figure 3. The measurement tube.

If the total pressure is measured in a boundary layer with the described cylindrical tube, it may be expected, that the disturbance caused by the measurement tube in the boundary layer is greater than when the measurement is carried out in a pitot tube, since in the latter only the mouth of the tube is located at the point to be studied. In particular in the cylindrical tube a disturbance will be noted by the fact that in the boundary layer the pressure along the stagnation line of the tube is not constant, but becomes smaller near the wall as a result of the decrease of the velocity. This circumstance will presumably cause in front of the tube a flow toward the wall, so that the flow lines of the boundary layer flow are deflected somewhat toward the wall, which led to the fact that the velocities in the boundary layer were measured somewhat too large, especially wherever the velocity gradient is large, that is, near the wall. To establish the differences between the indication of the cylindrical tube and that of a pitot tube, a velocity profile of a plane boundary layer was measured consecutively with both instruments. The graph in Fig. 4 shows that the cylindrical tube actually gives a somewhat too large velocity near the wall, on the other hand the velocity is somewhat too low in the external regions of the boundary layer. As may be seen from the graph, these errors are however not very large and they had to be accepted, since it hardly seems possible to introduce a correction, since its order of magnitude depends obviously from the corresponding variation of the velocity profile.

A measurement tube was attached to a shifting device, which makes it possible to shift it along the direction of its axis and to turn it around its axis. It was possible to measure the shift with a precision of 0.01 mm, and the rotation with a precision of

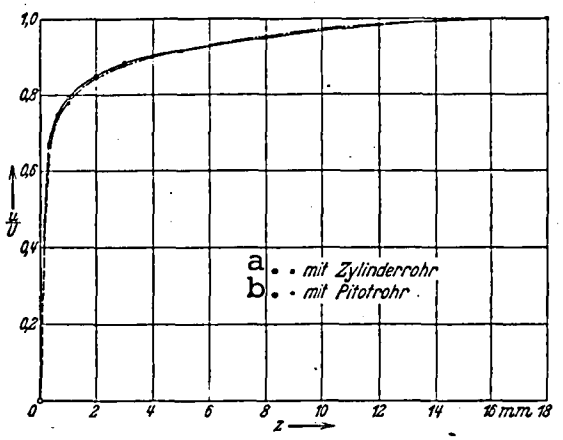

Figure 4. Comparative measurement between pitot tube and cylindrical tube.

Key: a. cylindrical tube
b. pitot tube

10'. This shifting device was screwed into the above mentioned hole located in the channel wall.

3. Measurement results. Figure 5 shows the measurement plate looking from below. The points at which the velocity profiles were measured are in the intersections of the lines indicated Roman and Arabic numbers. The lines designated with Roman numbers consist each of a straight line section and a curved arc, those designated by Arabic numbers are straight lines orthogonal to them. In Fig. 5 some flow lines on the potential flow are shown, plotted according to the measurements of angles with the cylindrical tube. In the shaded region there was no longer any potential flow; the boundary layers of the lower and upper channel wall ran into each other there. In the last portion of the channel only a small region with potential flow occurred. On the internal wall of the channel curvature the flow was torn off and specifically only in the central portion of the curved channel wall, whereas it was applied in the corners. This behavior which may appear remarkable at first glance is obviously to be attributed to the effect of the secondary flow, which continues from the upper and lower channel wall to the internal wall and causes a combined flow of the higher delayed air layers in the center of this wall. /358

The variation of the static pressure of the measurement plate is shown on Fig. 6. There the static pressure p refers to the total pressure g_o of the potential flow and measured on the pressure holes against the external chamber, is plotted over a series of cross sections.

Let the velocity of the potential flow be designated by U,

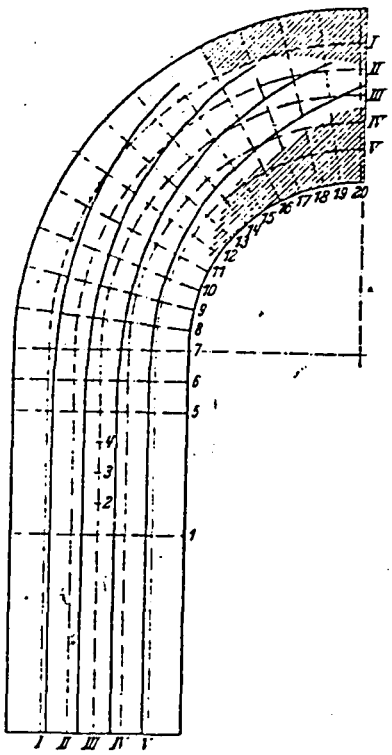

Figure 5. Measurement plate seen from below. The measurement points are at the intersections of the curves or straight lines designated by Roman or Arabic numbers. The solid line curves are flow lines of the potential flow.

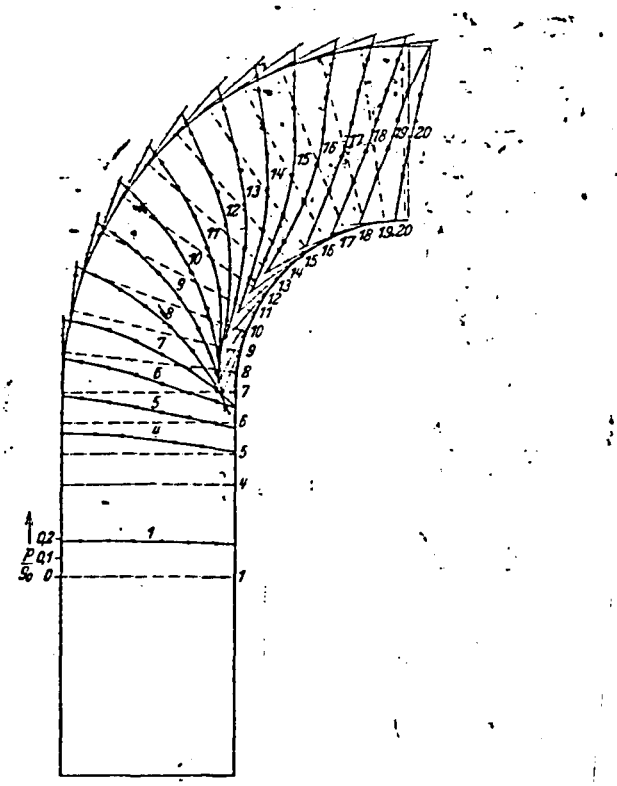

Figure 6. The static pressure on the measurement plate.

the component of the boundary layer flow in the direction of the potential flow by u, the one perpendicular to it by v. In so far as we are dealing with turbulent flows, we always refer to averages in time. Figure 7 shows as an example the velocity profile measured along the central line of a channel (line III in Fig. 5), and specifically the velocities u and v are referred to the potential velocity U occurring at the measurement point concerned, and /359 plotted over the distance z from the wall. Figure 8 shows the variation of a velocity at some point of line III as a polar diagram, while the heights z are indicated in millimeters at individual points.

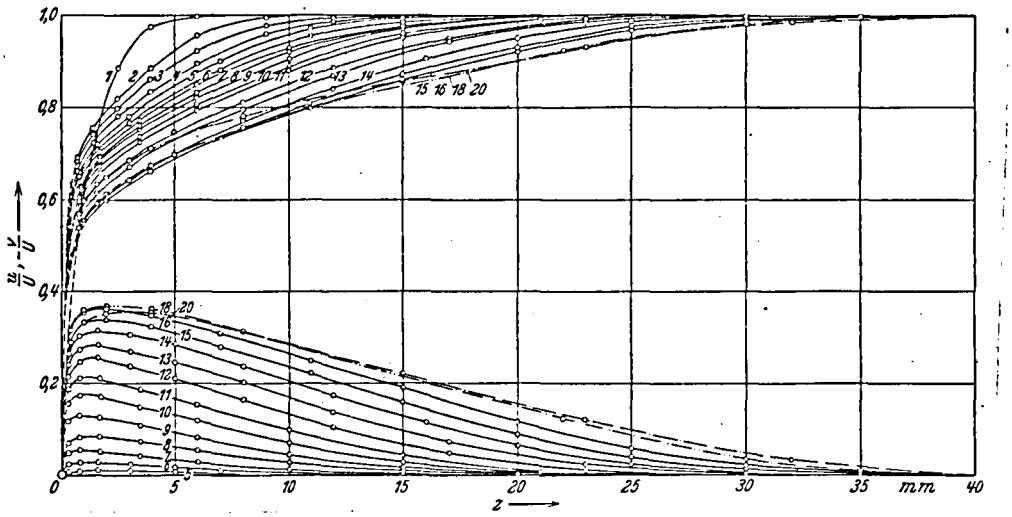

Figure 7. Velocity profile along the central line of a channel (Curve III in Fig. 5). The numbers on the profiles correspond to the designations in Fig. 5.

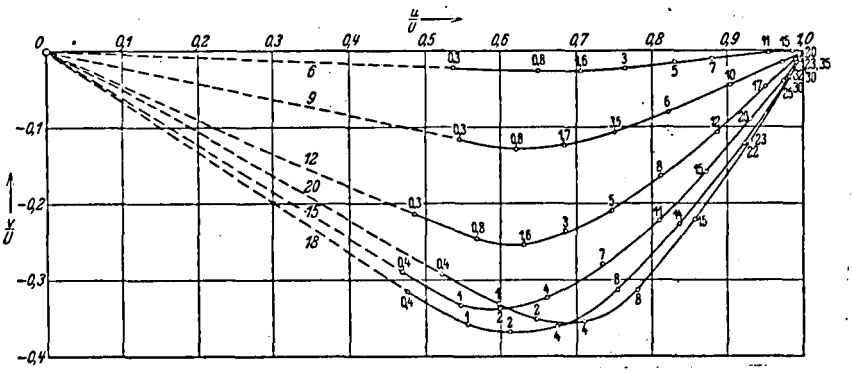

Figure 8. Polar diagram of the velocity at the measurement points 6, 9, 12, 15, 18 and 20 of Line III. The distances z from the wall are indicated in millimeters at the individual points.

Let U_o designate the potential velocity, corresponding to the static pressure p=0. Therefore we have $\frac{1}{2}\sigma U_0^2 = g_o$. The value U_o is essentially the velocity with which the potential flow leaves the channel. In the described measurements we have U_o=13.2 m/sec.

II. Application of the Pulse Equation to the Boundary Layer with Secondary Flow

1. Transformation of equations of motion. The hydrodynamic equations of motion will be converted as follows: let us imagine a flow line of the potential flow projected perpendicularly to the wall on which the boundary layer is located. Let x be the arc length along this projection, let y be the distance of the normal to it lying in the wall, and z the perpendicular distance from the wall. The equations of motion converted in this system apply in the vicinity of a cylindrical surface lying perpendicular to the wall and placed through the potential flow line concerned. Let X, Y, Z be the coordinates in a rectangular system of ordinates, whose (X, Y) plane coincides with the wall. It is apparent from Fig. 9 that the following equations of conversion apply: /360

$$\left.\begin{aligned} X &= \int_0^x \cos\alpha\, dx - y\sin\alpha, \\ Y &= Y_1 + y\cos\alpha, \\ Z &= z. \end{aligned}\right\} \qquad (1)$$

Here Y_1 is the ordinate of the projection of the potential flow line and α the angle between the tangent to this curve and the X axis. Both Y_1 and α are here to be considered as functions of the arc x. The curvature of the curve is designated by k. We have $k = \frac{d\alpha}{dx}$.

By differentiation we obtain from (1)

$$\begin{aligned} &\frac{\partial X}{\partial x} = (1 - yk)\cos\alpha, && \frac{\partial X}{\partial y} = -\sin\alpha, && \frac{\partial X}{\partial z} = 0, \\ &\frac{\partial Y}{\partial x} = (1 - yk)\sin\alpha, && \frac{\partial Y}{\partial y} = \cos\alpha, && \frac{\partial Y}{\partial z} = 0, \\ &\frac{\partial Z}{\partial x} = 0, && \frac{\partial Z}{\partial y} = 0, && \frac{\partial Z}{\partial z} = 1. \end{aligned}$$

We obtain thus for the functional determinant D

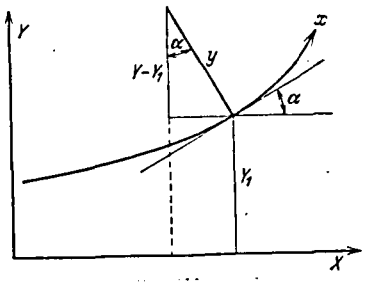

Figure 9.

$$D = \begin{vmatrix} \frac{\partial X}{\partial x} & \frac{\partial X}{\partial y} & \frac{\partial X}{\partial z} \\ \frac{\partial Y}{\partial x} & \frac{\partial Y}{\partial y} & \frac{\partial Y}{\partial z} \\ \frac{\partial Z}{\partial x} & \frac{\partial Z}{\partial y} & \frac{\partial Z}{\partial z} \end{vmatrix} = 1 - yk$$

and consequently for the derivatives of the inverse functions:

$$\left.\begin{array}{lll} \frac{\partial x}{\partial X} = \frac{\cos\alpha}{1-yk}, & \frac{\partial x}{\partial Y} = \frac{\sin\alpha}{1-yk}, & \frac{\partial x}{\partial Z} = 0, \\ \frac{\partial y}{\partial X} = -\sin\alpha, & \frac{\partial y}{\partial Y} = \cos\alpha, & \frac{\partial y}{\partial Z} = 0, \\ \frac{\partial z}{\partial X} = 0, & \frac{\partial z}{\partial Y} = 0, & \frac{\partial z}{\partial Z} = 1. \end{array}\right\} \qquad (2)$$

The equations of motion in the rectangular system of coordinates X, Y, Z are:

$$\begin{aligned} \varrho\left(u_0\frac{\partial u_0}{\partial X} + v_0\frac{\partial u_0}{\partial Y} + w_0\frac{\partial u_0}{\partial Z}\right) &= \frac{\partial \sigma_X}{\partial X} + \frac{\partial \tau_{XY}}{\partial Y} + \frac{\partial \tau_{XZ}}{\partial Z} - \frac{\partial p}{\partial X}, \\ \varrho\left(u_0\frac{\partial v_0}{\partial X} + v_0\frac{\partial v_0}{\partial Y} + w_0\frac{\partial v_0}{\partial Z}\right) &= \frac{\partial \sigma_Y}{\partial Y} + \frac{\partial \tau_{YZ}}{\partial Z} + \frac{\partial \tau_{XY}}{\partial X} - \frac{\partial p}{\partial Y}, \\ \varrho\left(u_0\frac{\partial w_0}{\partial X} + v_0\frac{\partial w_0}{\partial Y} + w_0\frac{\partial w_0}{\partial Z}\right) &= \frac{\partial \sigma_Z}{\partial Z} + \frac{\partial \tau_{XZ}}{\partial X} + \frac{\partial \tau_{YZ}}{\partial Y} - \frac{\partial p}{\partial Z}. \end{aligned}$$

Moreover we have the equation of continuity:

$$\frac{\partial u_0}{\partial X} + \frac{\partial v_0}{\partial Y} + \frac{\partial w_0}{\partial Z} = 0.$$

Here the velocities in the X, Y, Z directions are designated by u_0, v_0 and w_0, the density by σ, the static pressure by p and the matrix of the (apparent) friction stresses by

$$\begin{pmatrix} \sigma_X & \tau_{XY} & \tau_{XZ} \\ \tau_{XY} & \sigma_Y & \tau_{YZ} \\ \tau_{XZ} & \tau_{YZ} & \sigma_Z \end{pmatrix}.$$

We obtain with formula (2) after some calculation, the transformed equations of motion:

$$\left.\begin{aligned}
&\varrho\left(\frac{u}{1-yk}\frac{\partial u}{\partial x}+v\frac{\partial u}{\partial y}+w\frac{\partial u}{\partial z}\right)-\varrho uv\frac{k}{1-yk}=\\
&\qquad=\frac{\partial\sigma_x}{\partial x}\frac{1}{1-yk}+\frac{\partial\tau_{xy}}{\partial y}+\frac{\partial\tau_{xz}}{\partial z}-\frac{2\tau_{xy}k}{1-yk}-\frac{1}{1-yk}\frac{\partial p}{\partial x},\\
&\varrho\left(\frac{u}{1-yk}\frac{\partial v}{\partial x}+v\frac{\partial v}{\partial y}+w\frac{\partial v}{\partial z}\right)+\varrho u^2\frac{k}{1-yk}=\\
&\qquad=\frac{\partial\sigma_y}{\partial y}+\frac{1}{1-yk}\frac{\partial\tau_{xy}}{\partial x}+\frac{\partial\tau_{yz}}{\partial z}+\frac{(\sigma_x-\sigma_y)k}{1-yk}-\frac{\partial p}{\partial y},\\
&\varrho\left(u\frac{\partial w}{\partial x}+v\frac{\partial w}{\partial y}+w\frac{\partial w}{dz}\right)=\frac{\partial\sigma_z}{\partial z}+\frac{1}{1-yk}\frac{\partial\tau_{xz}}{\partial x}+\frac{\partial\tau_{yz}}{\partial y}-\frac{\tau_{yz}k}{1-yk}-\frac{\partial p}{\partial z},
\end{aligned}\right\}\qquad(3)$$

/361

and moreover the equation of continuity

$$\frac{1}{1-yk}\frac{\partial u}{\partial x}+\frac{\partial v}{\partial y}+\frac{\partial w}{\partial z}-\frac{vk}{1-yk}=0.$$

Here u, v, w are the velocities in the s, y, and z direction and

$$\begin{pmatrix}\sigma_x & \tau_{xy} & \tau_{xz}\\ \tau_{xy} & \sigma_y & \tau_{yz}\\ \tau_{xz} & \tau_{yz} & \sigma_z\end{pmatrix}$$

the matrix of the friction stresses in the (x, y, z) system of coordinates. The transition from the friction stresses in the (X, Y, Z) system to those in the (x, y, z) system is here given by the matrix equation

$$\begin{aligned}
\begin{pmatrix}\sigma_X & \tau_{XY} & \tau_{XZ}\\ \tau_{XY} & \sigma_Y & \tau_{YZ}\\ \tau_{XZ} & \tau_{YZ} & \sigma_Z\end{pmatrix}&=\begin{pmatrix}\cos(xX), & \cos(yX), & \cos(zX)\\ \cos(xY), & \cos(yY), & \cos(zY)\\ \cos(xZ), & \cos(yZ), & \cos(zZ)\end{pmatrix}\cdot\begin{pmatrix}\sigma_x & \tau_{xy} & \tau_{xz}\\ \tau_{xy} & \sigma_y & \tau_{yz}\\ \tau_{xz} & \tau_{yz} & \sigma_z\end{pmatrix}\times\\
&\times\begin{pmatrix}\cos(xX), & \cos(xY), & \cos(xZ)\\ \cos(yX), & \cos(yY), & \cos(xZ)\\ \cos(zX), & \cos(zY), & \cos(zZ)\end{pmatrix}=\\
&=\begin{pmatrix}\cos\alpha, & -\sin\alpha, & 0\\ \sin\alpha, & \cos\alpha, & 0\\ 0 & 0 & 1\end{pmatrix}\begin{pmatrix}\sigma_x & \tau_{xy} & \tau_{xz}\\ \tau_{xy} & \sigma_y & \tau_{yz}\\ \tau_{xz} & \tau_{yz} & \sigma_z\end{pmatrix}\begin{pmatrix}\cos\alpha, & \sin\alpha, & 0\\ -\sin\alpha, & \cos\alpha, & 0\\ 0 & 0 & 1\end{pmatrix}
\end{aligned}$$

where (xX) designates the angle between the x and X direction, (yX) the angle between the y and X direction etc.

2. The pulse equation. We will now integrate the first of equations (3) for y=0 over z, assuming that the static pressure

is independent of z inside the boundary layer. Of the friction terms here only $\partial\tau_{xz}/\partial z$ can be maintained, since in the boundary layer the other friction terms are small as compared with this. With this omission and for y=0, the first equation of motion is:

$$u\frac{\partial u}{\partial x}+v\frac{\partial u}{\partial y}+w\frac{\partial u}{\partial z}-uvk=\frac{1}{\varrho}\frac{\partial\tau_{xz}}{\partial z}-\frac{1}{\varrho}\frac{\partial p}{\partial x} \tag{4}$$

and the equation of continuity

$$\frac{\partial u}{\partial x}+\frac{\partial v}{\partial y}+\frac{\partial w}{\partial z}-vk=0. \tag{5}$$

Equation (4) is converted into

$$\frac{1}{2}\frac{\partial u^2}{\partial x}+\frac{\partial uv}{\partial y}-u\frac{\partial v}{\partial y}+\frac{\partial uw}{\partial z}-u\frac{\partial w}{\partial z}-uvk=\frac{1}{\varrho}\frac{\partial\tau_{xz}}{\partial z}-\frac{1}{\varrho}\frac{\partial p}{\partial x}.$$

In this equation we replace $\frac{\partial w}{\partial z}$ by the expression which is obtained for it (5) and we now have

$$\frac{\partial u^2}{\partial x}+\frac{\partial uv}{\partial y}+\frac{\partial uw}{\partial z}-2uvk=\frac{1}{\varrho}\frac{\partial\tau_{xz}}{\partial z}-\frac{1}{\varrho}\frac{\partial p}{\partial x}.$$

This equation integrated over z gives /364

$$\frac{\partial}{\partial x}\int_0^c u^2\,dz+\frac{\partial}{\partial y}\int_0^c uv\,dz+UW-2k\int_0^c uv\,dz=-\frac{1}{\varrho}\tau_{xz}^{(0)}-\frac{c}{\varrho}\frac{\partial p}{\partial x}. \tag{6}$$

Here c is a constant length, which is so large that for z=c, potential flow is present practically everywhere (therefore $\tau_{xz}=0$), $\tau_{xz}^{(0)}$ is the value of τ_{xz} (shear stress in the x direction) on the wall, and U and W designate the x and z components respectively of the potential velocity. We obtain for W by integration of equation (5) over z

$$W=k\int_0^c v\,dz-\frac{\partial}{\partial x}\int_0^c u\,dz-\frac{\partial}{\partial y}\int_0^c v\,dz. \tag{7}$$

According to the Bernoulli equation we have

	X_1 (cm)	$\frac{U}{U_0}$	$\frac{1}{U}\frac{\partial U}{\partial x}\cdot 10^3$ (1/cm)	$\frac{1}{U}\frac{\partial U}{\partial y}\cdot 10^3$ (1/cm)	φ_0	ϑ_x (mm)	ϑ_y (mm)	ϑ_{xy} (mm)	δ_x (mm)	δ_y (mm)	$\frac{\partial \vartheta_x}{\partial x}\cdot 10^3$	$\frac{\partial \vartheta_{xy}}{\partial y}\cdot 10^3$	$\frac{1}{U}\frac{\partial U}{\partial x}(2\vartheta_x + \frac{\tau_{xx}^{(m)}}{\varrho U^2}\cdot 10^3$ $+\delta_x)\cdot 10^3$		$0{,}01255\cdot\left(\frac{r}{U\vartheta_x}\right)^{\frac{1}{4}}\cdot 10^3$
								I							
5	84,00	0,847	− 1,30	− 2,26	0° 0′	1,30	0,00	0,00	1,88	0,00	2,1	0,1	− 0,6	1,6	2,23
6	92,00	0,834	− 3,13	− 3,51	1° 10′	1,55	0,00	− 0,02	2,19	− 0,07	3,0	0,4	− 1,6	1,8	2,16
7	100,00	0,809	− 3,65	− 4,49	3° 20′	1,85	0,00	− 0,05	2,57	− 0,17	4,5	0,2	− 2,3	2,4	2,08
8	109,66	0,784	− 2,55	− 7,10	9° 20′	2,36	0,04	− 0,18	3,36	− 0,71	5,8	− 1,5	− 2,2	2,1	1,98
9	119,33	0,768	− 2,26	− 7,08	16° 10′	3,05	0,18	− 0,44	4,42	− 1,47	7,5	− 3,9	− 2,4	1,2	1,86
10	128,99	0,756	− 1,62	− 7,87	23° 10′	3,60	0,38	− 0,75	5,30	− 2,39	5,8		− 2,0		
11	138,65	0,754	− 1,01	− 9,60	27° 30′	3,92	0,62	− 0,96	5,63	− 3,31	3,7		− 1,4		
12	148,32	0,755	− 1,33	− 10,8	29° 10′	3,99	0,82	− 1,09	5,49	− 4,16	− 0,6		− 1,8		
13	157,98	0,756	− 1,61	− 11,7	30° 10′	3,77	0,99	− 1,10	5,14	− 4,68			− 2,0		
14	167,64	0,756	− 1,67	− 11,9	28° 50′	3,48	1,09	− 1,03	4,67	− 5,03			− 1,9		
15	177,31	0,764	− 1,40	− 12,2	27° 30′	3,16	1,09	− 0,89	4,12	− 5,03			− 1,5		
16	186,97	0,760	− 0,70	− 12,7	26° 20′	3,03	1,11	− 0,85	3,94	− 5,12			− 0,7		
								II							
5	84,00	0,862	− 0,55	− 2,39	0° 10′	1,25	0,00	− 0,01	1,74	− 0,04	2,2	0,0	− 0,2	2,0	2,26
6	92,00	0,854	− 1,20	− 3,59	1° 50′	1,46	0,00	− 0,03	2,03	− 0,12	2,2	0,2	− 0,6	1,8	2,18
7	100,00	0,835	− 1,90	− 6,01	4° 10′	1,60	0,00	− 0,06	2,22	− 0,27	2,6	0,2	− 1,0	1,8	2,14
8	108,83	0,822	− 1,23	− 6,86	8° 10′	1,89	0,03	− 0,14	2,64	− 0,61	3,5	0,0	− 0,8	2,7	2,06
9	117,67	0,811	− 1,65	− 8,74	12° 50′	2,20	0,10	− 0,27	3,07	− 1,10	3,9	− 1,0	− 1,2	1,7	1,99
10	126,50	0,803	− 0,70	− 10,61	17° 40′	2,59	0,22	− 0,43	3,65	− 1,77	4,9	− 2,2	− 0,9	1,8	1,92
11	135,33	0,805	− 0,83	− 9,50	22° 20′	2,97	0,41	− 0,64	4,20	− 2,52	6,4	− 3,7	− 0,8	1,9	1,86
12	144,17	0,806	− 1,01	− 8,27	28° 0′	3,59	0,71	− 0,97	5,17	− 3,62	6,7		− 1,2		
13	153,00	0,809	− 1,03	− 8,72	31° 10′	3,93	1,09	− 1,28	5,68	− 4,77	6,4		− 1,4		
14	161,83	0,816	− 0,80	− 10,3	33° 50′	4,23	1,36	− 1,45	5,99	− 5,39	4,5		− 1,1		
15	170,67	0,823	− 0,21	− 9,7	35° 0′	4,28	1,72	− 1,56	5,91	− 6,31			− 0,3		
16	179,50	0,834	− 0,70	− 9,8	35° 0′	4,14	1,91	− 1,49	5,61	− 6,74			− 1,0		
17	188,33	0,845	− 0,71	− 9,4	35° 0′	4,06	1,94	− 1,47	5,55	− 6,87			− 1,0		
18	197,17	0,868	1,32	− 9,1	32° 40′	4,00	1,85	− 1,44	5,39	− 7,18			1,8		
19	206,00	0,907	3,68	− 7,9	31° 20′	3,84	1,65	− 1,32	4,94	− 7,18			4,6		
20	214,83	0,961	5,55	− 5,2	28° 20′	3,67	1,33	− 1,15	4,79	− 6,98			6,7		
								III							
5	84,00	0,876	0,04	− 2,31	0° 40′	1,38	0,00	− 0,01	1,94	− 0,05	—	0,0	0,0	—	2,20
6	92,00	0,877	− 0,03	− 3,26	2° 10′	1,61	0,00	− 0,05	2,20	− 0,18	1,2	0,0	0,0	1,2	2,11
7	100,00	0,875	− 0,18	− 6,79	5° 0′	1,69	0,00	− 0,07	2,27	− 0,34	1,2	0,0	0,0	1,2	2,09
8	108,00	0,868	0,09	− 8,68	7° 30′	1,81	0,03	− 0,15	2,46	− 0,68	1,8	− 0,1	0,0	1,7	2,06
9	116,01	0,867	− 0,30	− 9,77	14° 10′	1,96	0,10	− 0,21	2,70	− 1,07	2,4	− 0,5	− 0,2	1,7	2,04

10	124,01	0,866	−0,51	−10,3	16° 30′	2,17	0,19	−0,36	2,94	−1,58	2,6	−1,0	−0,4	1,2	1,97
11	132,01	0,865	−0,89	−11,2	20° 0′	2,32	0,31	−0,46	3,15	−2,07	3,0	−1,3	−0,7	1,0	1,94
12	140,02	0,863	−1,04	−11,2	24° 0′	2,65	0,49	−0,64	3,68	−2,78	3,5	−1,3	−0,9	1,3	1,88
13	148,02	0,869	−0,59	−11,2	26° 30′	2,86	0,70	−0,80	3,99	−3,52	4,4	−2,6	−0,6	1,2	1,84
14	156,02	0,875	−0,88	−10,6	29° 30′	3,28	0,93	−1,04	4,57	−4,24	5,2	−2,4	−1,0	1,8	1,77
15	164,03	0,880	−1,17	−10,2	31° 50′	3,56	1,18	−1,22	5,00	−5,03	4,8	−2,4	−1,4	1,0	1,75
16	172,03	0,890	0,00	−9,8	34° 20′	3,75	1,41	−1,41	5,17	−5,75	3,1		0,0		
17	180,03	0,903	−0,41	−10,2	34° 20′	3,83	1,50	−1,41	5,31	−5,92	2,4		0,0		
18	188,04	0,920	0,28	−9,0	33° 50′	3,92	1,68	−1,49	5,41	−6,53	2,2		0,4		
19	196,04	0,946	1,30	−6,7	31° 30′	4,00	1,67	−1,41	5,42	−6,48			1,8		
20	204,04	0,978	2,75	−4,2	26° 30′	3,82	1,67	−1,33	5,08	−6,64			3,5		
								IV							
5	84,00	0,893	1,46	−2,36	0° 30′	1,24	0,00	−0,01	1,74	−0,04	1,4	0,0	0,6	2,0	2,24
6	92,00	0,906	1,49	−4,09	2° 0′	1,38	0,00	−0,03	1,93	−0,10	2,3	−0,2	0,7	2,8	2,18
7	100,00	0,916	1,95	−6,42	5° 10′	1,59	0,00	−0,07	2,18	−0,32	2,5	−0,2	1,0	3,3	2,10
8	107,17	0,925	1,46	−10,2	8° 50′	1,80	0,04	−0,14	2,45	−0,66	2,8	−0,4	0,9	3,3	2,04
9	114,35	0,930	0,79	−11,1	13° 0′	2,01	0,09	−0,24	2,69	−1,05	2,9	−0,5	0,5	2,9	1,97
10	121,52	0,938	0,10	−11,8	17° 30′	2,20	0,21	−0,35	3,00	−1,67	2,7	−0,9	0,1	1,9	1,93
11	128,69	0,940	−0,77	−12,9	20° 10′	2,37	0,33	−0,47	3,21	−2,11	2,5		−0,6		
12	135,87	0,943	−0,74	−13,2	24° 40′	2,58	0,50	−0,62	3,50	−2,74	2,5		−0,6		
13	143,04	0,948	−1,27	−13,5	27° 20′	2,70	0,68	−0,75	3,70	−3,33	2,3		−1,1		
14	150,21	0,951	−1,55	−12,9	29° 0′	2,83	0,87	−0,88	3,91	−3,89	2,8		−1,5		
15	157,39	0,951	−1,61	−12,6	32° 0′	3,08	1,08	−1,06	4,22	−4,53	3,0		−1,7		
16	164,56	0,956	−1,57	−11,7	33° 10′	3,22	1,26	−1,19	4,50	−5,09	3,5		−1,7		
17	171,73	0,966	−1,64	−9,4	33° 10′	3,30	1,36	−1,21	4,54	−5,31	3,8		−1,8		
18	178,91	0,971	−1,26	−7,7	33° 10′	3,42	1,50	−1,32	4,77	−5,82			−1,5		
								V							
5	84,00	0,906	3,04	−2,01	1° 0′	1,11	0,00	−0,01	1,49	−0,04	0,8	0,0	1,1	1,9	2,30
6	92,00	0,930	4,07	−3,38	1° 20′	1,18	0,00	−0,02	1,63	−0,06	0,9	−0,2	1,6	2,3	2,26
7	100,00	0,965	5,22	−7,85	4° 30′	1,24	0,00	−0,05	1,67	−0,27	0,6	−0,4	2,2	2,4	2,20
8	106,34	0,991	3,68	−11,6	8° 20′	1,32	0,03	−0,11	1,76	−0,55	1,2	−0,5	1,6	2,3	2,16
9	112,69	1,010	2,23	−13,1	11° 20′	1,42	0,07	−0,15	1,88	−0,82	1,4	−0,5	1,0	1,9	2,11
10	119,03	1,025	1,64	−13,3	16° 0′	1,55	0,14	−0,23	2,05	−1,17			0,8		
11	125,37	1,038	0,2	−15,8	20° 0′	1,68	0,23	−0,33	2,25	−1,55			0,1		
12	131,72	1,040	−1,1	−14,7	24° 30′	1,91	0,37	−0,45	2,60	−2,14			−0,7		
13	138,06	1,043	−1,7	−13,9	26° 20′	2,06	0,53	−0,59	2,88	−2,69			−1,2		
14	144,40	1,042	−1,9	−13,7	28° 50′	2,27	0,67	−0,71	3,16	−3,13			−1,5		

The Roman and Arabic numbers, designating the measurement points, correspond to the designations in Fig. 5. X_1 is the distance of the measurement points from the front edge of the measurement plate, measured on the lines designated in Fig. 5 with Roman numerals. Distances between the lines are 7 cm. ϕ_0 is the angle which is formed by the boundary flow line on the wall with the direction of the potential velocity. The angle ϕ_0 is obtained by extrapolation of the angle measured with the cylindrical tube.

$$\frac{\partial p}{\partial x} = -\rho U \frac{dU}{dx}.$$

We may also write for it

$$\frac{\partial p}{\partial x} = U \frac{\partial}{\partial x}\int_0^\delta U\,dz - \frac{\partial}{\partial x}\int_0^\delta U^2\,dz. \tag{8}$$

Moreover we obtain for the curvature of the potential flow line

$$k = \frac{1}{U}\frac{\partial U}{\partial y}, \tag{9}$$

as obtained from the second of equations (3) together with the Bernoulli equation.

If (7), (8) and (9) are introduced into (6), we obtain finally

$$\frac{\partial}{\partial x}\int_0^\delta (U-u)u\,dz + \frac{\partial U}{\partial x}\int_0^\delta (U-u)\,dz + \frac{\partial}{\partial y}\int_0^\delta (U-u)v\,dz - \frac{1}{U}\frac{\partial U}{\partial y}\int_0^\delta (U-u)v\,dz = \frac{\tau_0}{\rho}. \tag{10}$$

Now the following designations may be introduced:

$$\vartheta_1 = \frac{1}{U^2}\int_0^\delta (U-u)u\,dz, \quad \vartheta_2 = \frac{1}{U^2}\int_0^\delta (U-u)v\,dz, \quad \delta_1 = \frac{1}{U}\int_0^\delta (U-u)\,dz.$$

With these designations we obtain from (10)

$$\frac{\partial \vartheta_1}{\partial x} + \frac{1}{U}\frac{\partial U}{\partial x}(2\vartheta_1 + \delta_1) + \frac{\partial \vartheta_2}{\partial y} = \frac{\tau_0}{\rho U^2}. \tag{11}$$

This equation may be called the "pulse equation". It is a generalization of the equation valid for friction layers in a plane flow, which was first derived by Karman by applying the pulse flow to the friction layer or boundary layer[4].

For the sake of completeness we should also indicate the

[4] Th. v. Kármán, Z. angew. Math. Mech. 1, 233 (1921).

corresponding integration valid for the y direction, although it is not used hereafter. It may be derived in the same way as equation (11) from the second part of Eq. (3) for y = 0 and disregarding the friction term except for $\frac{\partial \tau_{yz}}{\partial z}$, and becomes:

$$\frac{\partial \vartheta_y}{\partial y} + \frac{\partial (\delta_y - \vartheta_{xy})}{\partial x} + \frac{1}{U}\frac{\partial U}{\partial y}(\vartheta_y - \vartheta_x - \delta_x) + \frac{2}{U}\frac{\partial U}{\partial x}(\delta_y - \vartheta_{xy}) = -\frac{\tau_{yz}^{(0)}}{\varrho U^2}.$$

Here the designations

$$\vartheta_y = \frac{1}{U^2}\int_0^\infty v^2\, dz, \qquad \delta_y = \frac{1}{U}\int_0^\infty v\, dz$$

are further introduced and $\tau_{yz}^{(0)}$ is the value of τ_{yz} of the wall.

3. Application of the pulse equation to the measured velocity profile. /365 In the above Table the values of θ_x, θ_y, θ_{xy}, δ_x and δ_y obtained from the measured velocity profile are indicated. To give a survey of the order of magnitude of the individual elements of equation (11) the latter are also given in the Table. The derivatives in the three terms on the left side of equation (11) were established graphically from the values obtained with the measurements. It was possible to determine them only with rather high uncertainty, in particular, $\partial\theta_{xy}/\partial_y$ was extremely hard to establish. Wherever values are not indicated in the Table, it was impossible to determine the derivatives. The values obtained by addition of the three terms for $\tau_{xz}^{(0)}/\sigma U^2$ are to be considered only as estimated values. It is apparent from the Table that the term representing the effect of a secondary flow in (11) is of the same order of magnitude as the others.

For comparison the Table also gives the wall shear stresses, which would be present in a boundary layer in plane flow of the same thickness (same θ_x) for the same potential velocity. For the Reynold numbers occurring here, the assumption of a velocity distribution in which the velocity is proportional to the 7th root

of the distance from the wall, provides a sufficient approximation for these shear stresses. With this assumption we obtain for the shear stress τ_0 of the wall[5]

$$\frac{\tau_0}{\varrho U^2} = 0{,}01255 \left(\frac{\nu}{U \vartheta_x}\right)^{\frac{1}{4}}.$$

It is apparent from the Table that the values of shear stress obtained from the best measurements are spread around those in the plane flow.

Summary

The article describes measurements with an experimental equipment used to study the boundary layer on a plane wall, along which the flow occurs, whose potential flow lines are curved in plane parallel to the wall. According to the equation frequently applied to boundary layers in a plane flow, wich is usually obtained there by using the pulse law,a generalization is derived which is valid for boundary layers with spatial flow. The wall shear stresses were calculated with this equation.

[5]Compare v. Kármán, Loc. cit and E Gruschwitz, Ing.-Arch. 2, 341 (1931).

End of Document